Original Article

JCBFM

Journal of Cerebral Blood Flow & Metabolism
2019, Vol. 39(2) 240–250

DOI: 10.1177/0271678X17743670
journals.sagepub.com/home/jcbfm
SAGE

Experimental chronic cerebral hypoperfusion results in decreased pericyte coverage and increased blood–brain barrier permeability in the corpus callosum

Qinghai Liu[1], Ryan Radwanski[1], Robin Babadjouni[1], Arati Patel[1], Drew M Hodis[1], Peter Baumbacher[1], Zhen Zhao[1], Berislav Zlokovic[1] and William J Mack[1,2]

Abstract

Murine chronic cerebral hypoperfusion (CCH) results in white matter (WM) injury and behavioral deficits. Pericytes influence blood–brain barrier (BBB) integrity and cerebral blood flow. Under hypoxic conditions, pericytes detach from perivascular locations increasing vessel permeability and neuronal injury. This study characterizes the time course of BBB dysfunction and pericyte coverage following murine experimental CCH secondary to bilateral carotid artery stenosis (BCAS). Mice underwent BCAS or sham operation. On post-procedure days 1, 3, 7 and 30, corpus callosum BBB permeability was characterized using Evans blue (EB) extravasation and IgG staining and pericyte coverage/count was calculated. The BCAS cohort demonstrated increased EB extravasation on postoperative days 1 ($p = 0.003$) 3 ($p = 0.002$), and 7 ($p = 0.001$) when compared to sham mice. Further, EB extravasation was significantly greater ($p = 0.05$) at day 3 than at day 30 in BCAS mice. BCAS mice demonstrated a nadir in pericyte coverage and count on post-operative day 3 ($p < 0.05$, compared to day 7, day 30 and sham). Decreased pericyte coverage/count and increased BBB permeability are most pronounced on postoperative day 3 following murine CCH. This precedes any notable WM injury or behavioral deficits.

Keyword

Carotid stenosis, hypoperfusion, pericyte, permeability, white matter

Received 28 October 2016; Accepted 16 October 2017

Introduction

Multiple animal models exist to examine the pathophysiology and mechanisms of acute stroke.[1,2] However, few experimental systems recapitulate subtle ischemic injury resulting from chronic cerebral hypoperfusion (CCH). Cognitive injury secondary to cerebral hypoperfusion is pervasive and likely underrecognized. In the population-based Framingham study cohort, the prevalence of significant carotid stenosis (>50%) was reported to be 7% in women and 9% in men.[3] Clinical carotid endarterectomy studies of cerebral hypoperfusion demonstrate a nearly 25% incidence of subtle cognitive decline in the absence of overt neurologic change or radiographic evidence of stroke.[4] Neurodegenerative diseases such as Alzheimer's disease and vascular dementia have become increasingly more common as the population ages.[5–8] Epidemiologic risk factors for AD and vascular dementia are strongly associated with hypoperfusion and clinical

[1]Zilkha Neurogenetic Institute, Keck School of Medicine, University of Southern California, Los Angeles, CA, USA
[2]Department of Neurosurgery, Keck School of Medicine, University of Southern California, Los Angeles, CA, USA

Corresponding author:
William J Mack, Keck School of Medicine, University of Southern California, 1520 San Pablo Street, Suite 3800, Los Angeles, CA 90033, USA.
Email: William.Mack@med.usc.edu

symptomatology demonstrates significant overlap.[9] Many therapeutic agents designed to treat AD target cerebral hypoperfusion.[10] Determining the cellular processes that affect neuronal and white matter injury in the setting of CCH is critical to understanding the pathophysiology, temporal progression, and potential clinical implications of the process.

The neurovascular unit (NVU) is comprised of neurons, endothelial cells, microglia, astrocytes, pericytes, and an extracellular basement membrane.[11] In concert, these cells maintain homeostasis of the brain microvironment.[11] The blood–brain barrier (BBB) is regulated by transcytosis across endothelial cell membranes and tight junctions of the brain capillaries.[12] Pericytes play a critical role in BBB integrity and regulation of cerebral blood flow (CBF).[13] In the setting of cerebral hypoxia, pericytes detach from their perivascular locations resulting in BBB disruption, microvascular permeability, and secondary neuronal injury.[14] The pericyte response to CCH has not been characterized.

This study leverages an experimental murine bilateral carotid artery stenosis (BCAS) model to examine the temporal pattern of BBB dysfunction and endothelial pericyte coverage in the setting of CCH. The model consistently demonstrates mild white matter ischemic injury in the corpus callosum, in conjunction with astrocyte and microglial upregulation, 30 days after initiation of CCH.[15–17] These pathological changes are associated with isolated neurocognitive deficits in working memory.

Methods

Animals

All procedures utilized in this study were approved by the Institutional Animal Care and Use Committee (IACUC; protocol # 11565) of the University of Southern California and carried out in accordance with the Guide for the Care and Use of Laboratory Animals (NIH). Animals were male C57BL/6J mice (9–11 weeks of age; ~24–29 g) and housed in a barrier facility with free access to food and water on a 12-h light dark cycle. Experiments were conducted and reported per the ARRIVE guidelines.

BCAS

A total of 24 mice underwent the BCAS procedure and 36 mice underwent sham surgery. Two control mice did not undergo a surgical procedure or anesthesia. The BCAS procedure was performed in accordance with prior publications[15,16,18] with minor modifications. After a seven-day quarantine period, mice were anesthetized with intraperitoneal ketamine/xylazine (10 µl/g) and placed in the prone position with rectal temperature maintained between 36.5°C and 37°C. A laser Doppler flowmetry (LDF) microtip fiber probe was affixed to the skull at 1 mm posterior and 5 mm left side lateral of the bregma. The mouse was then rotated to the supine position and CBF was recorded with a PF 5010 laser Doppler perfusion monitor (Perimed AB, Sweden). A midline cervical incision was made and both common carotid arteries (CCA) were exposed. A microcoil (inner diameter 0.18 mm, Sawane company, Japan) was placed around each CCA and CBF recording was obtained. Sham-operated animals underwent the same procedure excluding placement of the microcoils.

BBB permeability

Twelve BCAS and 12 sham mice were used for BBB permeability experiments. At post-procedure days 1, 3, 7, and 30 mice were given an IP injection of 2% Evans blue (EB; 10 µl/g; Sigma-Aldrich) 2 h before deeply anesthetizing with ketamine/xylazine (~300 µl). Visibility of Evans blue in the ears, paws, and tail indicated successful Evans blue administration (if absent mice were not included). At 2 h post Evans blue administration, anesthesia was administered followed by transcardial perfusion with chilled phosphate-buffered saline (PBS) containing 5 U/ml heparin and subsequent 4% paraformaldehyde. Tissue was embedded with OCT, cut into 20 µm sections, and co-stained with Hoechst 33,258 for 10 min. Integrate density was calculated in the corpus callosum. During image acquisition, all settings remained unchanged, and only images without saturated pixels were included for quantification. BBB permeability was quantified in the medial region of each side (right/ left) of the corpus callosum and the adjacent frontal cortex by two blinded, independent observers and averaged for a final value.

Pericyte coverage and count/BBB permeability

Immunofluorescence. Twelve BCAS ($n = 3$ for each time point) mice and 15 sham animals ($n = 3$ for day 1, $n = 4$ for days 3, 7, 30) were used in the assessment of pericyte coverage/count and occludin quantification. Three BCAS (day 30) and four sham mice (day 30) were used for the quantification of IgG. For pericyte coverage/count, occludin, and IgG experiments, mice were deeply anesthetized by an IP injection of a ketamine/xylazine (~300 µl) and transcardially perfused with chilled PBS containing 5 U/ml heparin followed by 4% paraformaldehyde at post-procedure days 1, 3, 7 and 30. Tissue was fixed in paraformaldehyde at 4°C overnight and then transferred into PBS buffer prior to embedding in 4% low gelling temperature

agarose (Sigma-Aldrich, MO), and cut into 40 μm sections by vibratome (Leicia). Tissue slices were placed in 24 well plates and blocked with 5% donkey serum. The samples were treated with primary antibodies CD13 [R&D AF2335][Pericyte marker], CD31 [BD 550274] [Endothelial marker], and PDGFR β [AB 32570 dilution 50 Rb] [Pericyte marker] and Occludin [Thermo Fisher 71-1500] [Tight junction marker] and left on an agitator at 4°C overnight. Lectin [Endothelial marker], anti-mouse IgG fluorescence and donkey anti-rabbit fluorescence were added and co-stained with DAPI. Finally, tissue sections were mounted and covered with glass.

Immunofluorescence analysis. All images were obtained with a Zeiss 510 confocal microscope and BZ-9000 fluorescent microscope (Keyence, NJ). Analysis was performed using NIH Image J software with Neuron J plugin. Images were taken from the right and left medial corpus callosum and the adjacent cerebral cortex. Sections were analyzed by two blinded, independent observers and subsequently averaged. The coverage of pericytes was determined by ratio of CD13 positive pericytes to CD31 positive capillaries (≤10 um in diameter). Pericyte count was determined by co-localizing DAPI positive nuclei with CD13 positive cells (expressed as mm^2) by merging the two images. Pericyte coverage was also determined on day 30 by PDGFR β/ CD31 ratio as a validation. The coverage of occludin was determined by the ratio of occludin positivity and lectin positive capillaries (≤10 um in diameter).

Statistical analysis. SPSS 23 software was used to analyze results. BCAS cohort differences were compared using ANOVA and post-hoc Tukey's multiple comparison tests. BCAS values were compared to mean sham values with two-tailed unpaired Student's *t* tests. Data are presented as mean±SEM. $p \leq 0.05$ is considered statistically significant.

Results

CBF

Mean CBF change in the Sham ($n = 21$) vs. BCAS ($n = 24$) cohort were as follows: Sham: $4.38\% \pm 12.85$; 0.18 mm BCAS (2nd coil): $-22.75\% \pm 14.70$. There was a significant difference in CBF drop-off between Sham operated and BCAS (2nd coil) mice ($p < 0.0001$).

BBB permeability in the corpus callosum

Summary of sham EB extravasation integrate densities in the medial region of the corpus callosum are as follows: Sham day 1, 11.74 ± 8.79, $n = 3$; Sham day 3, 121.66 ± 39.80, $n = 3$; Sham day 7, 48.31 ± 23.66, $n = 3$; Sham day 30, 8.92 ± 1.27, $n = 3$. The BCAS cohort demonstrated increased EB extravasation (integrate density) on postoperative days 1 [583.58 ± 98.28, $p = 0.003$, $n = 3$], day 3 [1529.32 ± 448.87, $p = 0.02$, $n = 3$] and day 7 [366.02 ± 34.51, $p = 0.001$, $n = 3$] when compared to the mean sham value at each corresponding time point. There were no differences in densities on day 30 [5.85 ± 1.80, $p = 0.14$, $n = 3$], when compared to day 30 sham values. Further, EB extravasation values were significantly different (ANOVA, $p = .009$) across all time points within the BCAS cohort. Specifically, the integrate densities were significantly greater at day 3 (peak level) than at day 7 and day 30 ($p < 0.05$) in BCAS mice. EB extravasation was apparent on gross brain specimen on BCAS postoperative day 3 (Figures 1 and 2(a) and (b)).

BBB permeability in the cerebral cortex

Summary of the Sham EB extravasation integrate densities in the cerebral cortex are as follows: Sham day 1, 13.33 ± 13.63, $n = 3$; Sham day 3, 160.04 ± 115.63, $n = 3$; Sham day 7, 57.31 ± 22.30, $n = 3$; Sham day 30, 8.83 ± 8.94, $n = 3$. The BCAS cohort demonstrated increased EB extravasation (integrate density) on postoperative day 1 [557.11 ± 210.20, $p = 0.01$, $n = 3$], day 3 [3398.22 ± 779.92, $p = 0.002$, $n = 3$] and day 30 [30.86 ± 9.29, $p = 0.04$, $n = 3$]. There was no difference in density on day 7 [261.92 ± 143.63, $p = 0.07$, $n = 3$]. EB extravasation values were significantly different (ANOVA, $p < 0.001$) across all time points within the BCAS cohort. Specifically, the integrate densities were greater at day 3 compared to day 1, 7 and 30 ($p < 0.05$) in BCAS mice (Figure 2(c) and (d)).

Extravascular IgG deposition in the corpus callosum

In order to determine qualitative positive IgG staining, images were taken from the left and right corpus callosum and subsequently averaged. IgG deposition is visibly increased at day 3 in the BCAS cohort; however, the difference is not statistically significant. Results for day 3 BCAS and Sham integrate densities are as follows: BCAS 53068 ± 45493 [mean ± SEM], $n = 3$; Sham 1927 ± 595.3 [mean ± SEM], $n = 3$, $p = 0.3239$ (Figure 2(e)).

Occludin coverage in the corpus callosum

BCAS occludin/microvessel coverage ratios in the corpus callosum did not show differences at any time point when compared to corresponding sham time points [day 1, $40.29 \pm 14.51\%$, $n = 3$, $p = 0.91$; day 3,

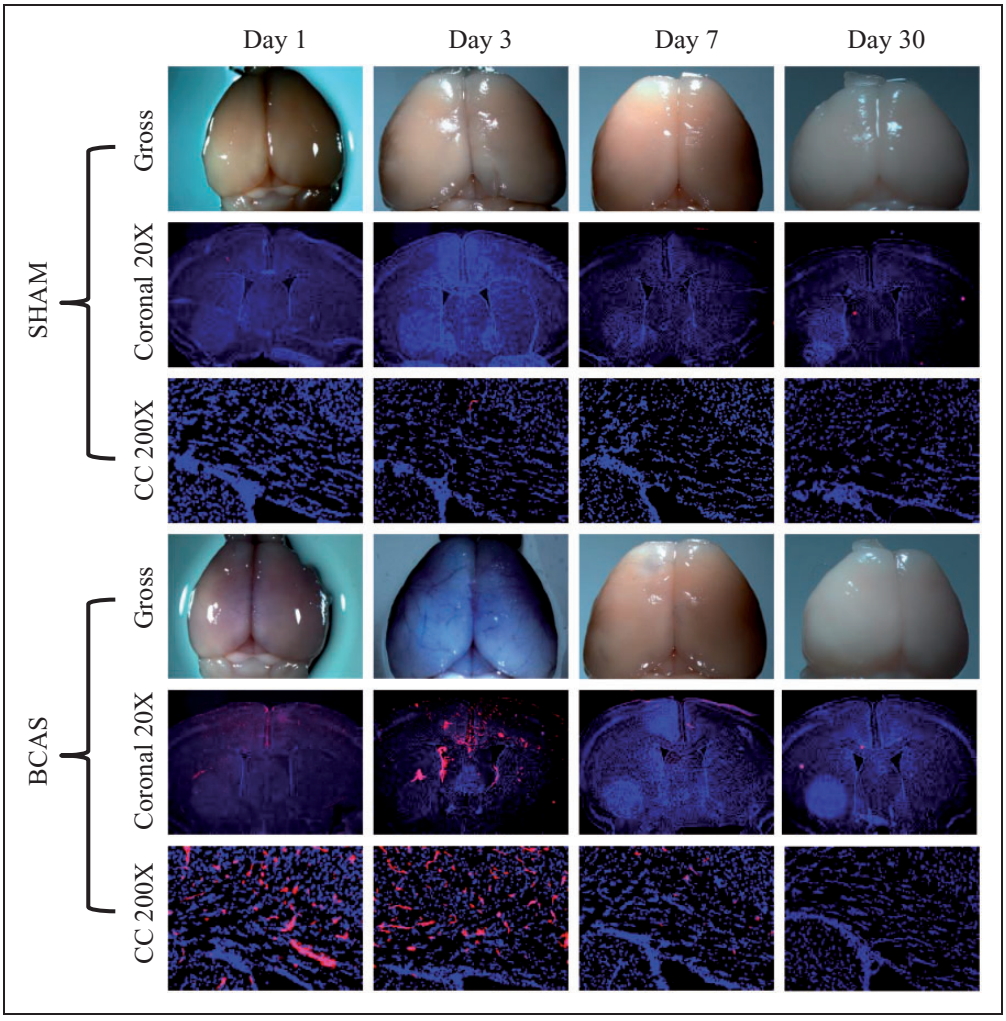

Figure 1. Blood–brain barrier permeability following BCAS. Evan blue staining for BBB permeability on postoperative days 1, 3, 7 and 30. Top: sham, bottom: BCAS. Blue is DAPI staining and pink Evans blue. Gross specimens (top), coronal slices (middle, 20×) and high magnification corpus callosum (bottom, 200×) are shown.

$41.60 \pm 8.73\%$, $p = 0.35$; day 7, $44.61 \pm 5.95\%$, $n = 3$, $p = 0.90$; day 30, $51.23 \pm 20.06\%$, $n = 3$, $p = 0.31$]. Further, no differences were found between BCAS time points [day 1 vs. day 3, $p = 0.90$; day 3 vs. day 7, $p = 0.64$; day 7 vs. day 30, $p = 0.61$]. Summary of sham occludin coverage ratios is as follows: [day 1, $41.78 \pm 16.21\%$, $n = 4$; day 3, $53.05 \pm 17.61\%$, $n = 4$; day 7, $43.64 \pm 11.55\%$, $n = 4$; day 30, $40.0 \pm 8.45\%$, $n = 4$] (see Figure 3(a) and (b))

Pericyte coverage and count in corpus callosum

Control (non-operative) mice showed a mean pericyte coverage ratio of $83.91 \pm 4.53\%$ ($n = 2$). The summary of sham pericyte coverage is as follows: Sham day 1, $71.28 \pm 6.16\%$, $n = 3$; Sham day 3, $86.04 \pm 2.33\%$, $n = 4$; Sham day 7, $75.56 \pm 5.57\%$, $n = 4$; Sham day 30, $91.63 \pm 8.10\%$, $n = 4$. The pericyte coverage ratios were significantly different in the BCAS cohort across all postoperative testing days (ANOVA $p = .001$). Specifically, the CCH mice demonstrated a nadir in pericyte coverage on post-operative day 3 ($30.88 \pm 10.27\%$, $n = 3$). Values on day 3 ($30.88 \pm 10.27\%$) were significantly lower than those on postoperative days 7 ($89.36 \pm 5.11\%$, $n = 3$; $p < 0.05$), and 30 ($74.97 \pm 2.39\%$, $n = 3$; $p < 0.05$). Pericyte coverage ratios on day 3 ($30.88 \pm 10.27\%$) were also significantly decreased compared to mean values of sham mice on day 3($86.04 \pm 2.33\%$; $n = 4$; $p = .002$). BCAS pericyte coverage values on day 7 ($89.36 \pm 5.11\%$, $n = 3$) were significantly greater than those on day 1 ($58.42 \pm 6.08\%$, $n = 3$; $p = .02$). PDGFRβ and CD13 staining co-localized on CD31 (vessels) DAPI positive nuclei in the corpus callosum

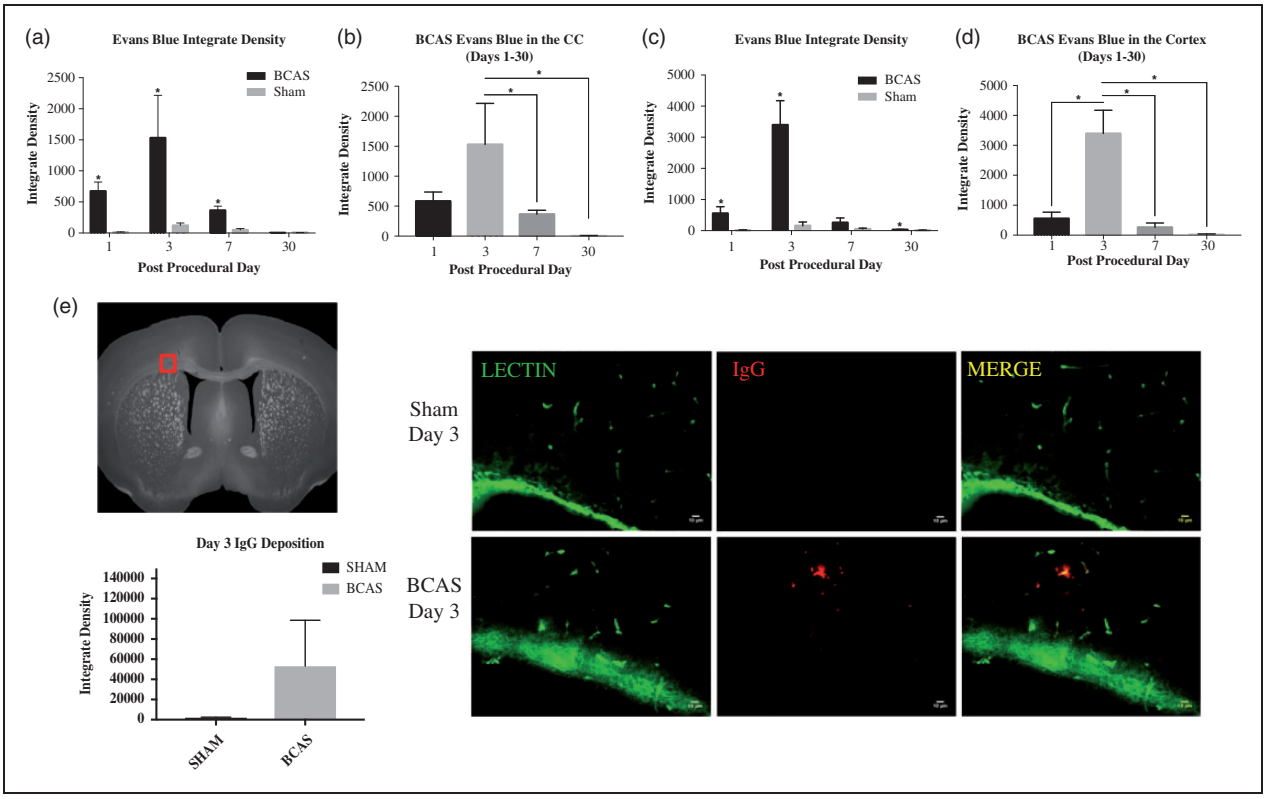

Figure 2. Evan blue integrate densities in the corpus callosum. (a) Values are depicted for BCAS and sham animals on days 1, 3, 7, 30. BCAS values are significantly higher on days 1, 3 and 7 when compared to the corresponding sham time point. (b) Densities were significantly greater in the BCAS cohort on day 3 when compared to day 7 and 30. * signifies $p < 0.05$. BCAS cohort (day 1, $n = 3$; day 3, $n = 3$; day 7, $n = 3$; day 30, $n = 3$). Sham cohort (day 1, $n = 3$; day 3, $n = 3$; day 7, $n = 3$; day 30, $n = 3$). Two sections were used per mouse. Sections were taken from the right and left medial corpus callosum. (c and d): Evans Blue integrate densities in the cortex. (c) Values are depicted for BCAS and sham animals on days 1, 3, 7, 30. BCAS values are significantly higher on days 1, 3, and 30 when compared to the corresponding sham time point. (d) Densities were significantly greater in the BCAS cohort on day 3 when compared to day 1, 7 and 30. BCAS cohort (day 1, $n = 3$; day 3, $n = 3$; day 7, $n = 3$; day 30, $n = 3$). Sham cohort (day 1, $n = 3$; day 3, $n = 3$; day 7, $n = 3$; day 30, $n = 3$). Two sections were used per mice. Sections were taken from the right and left cortex above the corpus callosum. (e) BBB permeability. Immunohistochemistry demonstrates perivascular IgG staining in the corpus callosum of BCAS animals on postoperative day 3 (middle, bottom). Negligible IgG positivity in sham animals. Statistical analysis shown with qualitatively increased although not statistically significant IgG deposition at day 3 ($p = 0.3239$) (left). Scale bar: 10 μm. Sections were obtained from the medial portion of the corpus callosum (left). Error bars represent standard error of the mean.

on postoperative day 30 sham and BCAS specimens (Figures 4, 5 and 6(a) and (b)).

The pericyte count in the corpus callosum was significantly different in the BCAS cohort across all postoperative testing days (ANOVA $p < 0.01$). The CCH mice demonstrated a nadir in pericyte count on postoperative day 3 (367.03 ± 151.40, $n = 3$). Values on day 3 (367.03 ± 151.40) were significantly lower than those on postoperative days 7 (925.61 ± 172.74, $n = 3$, $p < 0.01$), and 30 (831.25 ± 158.55, $n = 3$, $p < 0.05$). Pericyte count on day 3 (367.03 ± 151.40) was significantly decreased compared to mean values of sham mice on day 3 (836.39 ± 67.59, $n = 4$, $p = .01$). Summary of sham pericyte counts is as follows: sham day 1, 664.84, $n = 3$; sham day 3, 836.39, $n = 4$; sham day 7, 943.72, $n = 4$; day 30, 844.02 ± 88.70, $n = 4$) (Figure 6(c)).

Pericyte coverage in the cortex

BCAS pericyte/microvessel coverage ratios in the cortex demonstrated a significant decline at day 3 [$49.77 \pm 5.06\%$, $n = 3$, $p = .02$] when compared to the sham mice on day 3 [$72.22 \pm 3.09\%$; $n = 4$]. BCAS pericyte/microvessel coverage ratios significantly increased at day 7 [$84.38 \pm 9.61\%$, $n = 3$, $p = 0.02$] compared to the sham mice on day 7 [$62.40 \pm 5.11\%$; $n = 4$]. No differences were found in the BCAS pericyte/microvessel coverage ratios in the cortex for the remaining time points [day 1, $75.06 \pm 10.90\%$, $n = 3$, $p = 0.091$; day 30,

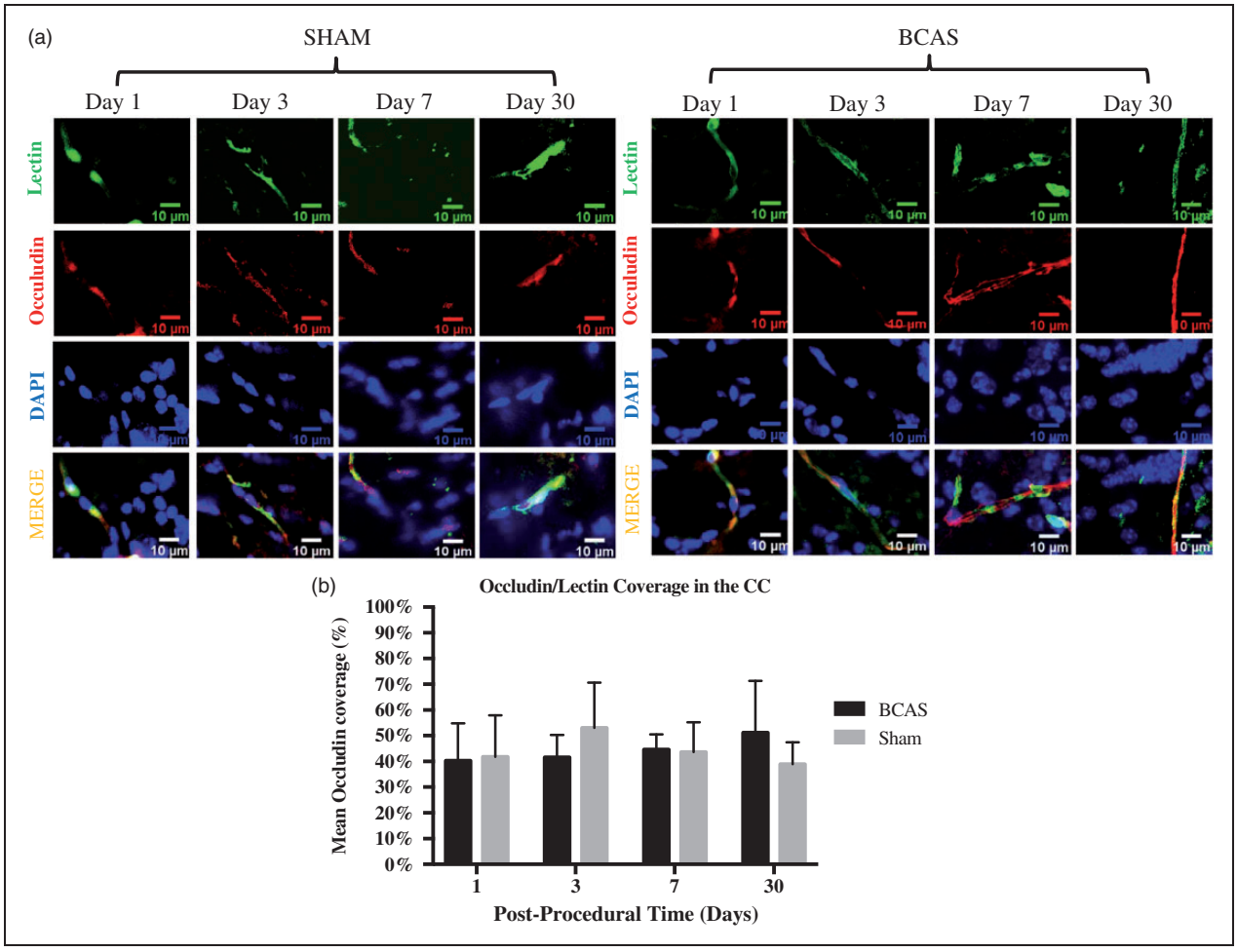

Figure 3. Tight junction integrity. (a) Occludin coverage in the corpus callosum on post-operative days 1, 3, 7 and 30. Left: Sham, right: BCAS. Representative lectin (green), occludin (red), DAPI (blue) and merged sections (yellow) at each time point. Scale bar: 10 μm. (b) Occludin coverage bar graph. Values are depicted for BCAS and sham animals on days 1, 3, 7 and 30. No significant difference exists between BCAS and sham animals at all time points. No significant difference exists among BCAS animals at all time points. BCAS cohort (day 1, $n=3$; day 3, $n=3$; day 7, $n=3$; day 30, $n=3$). Sham cohort (day 1, $n=4$; day 3, $n=4$; day 7, $n=4$; day 30, $n=4$). Two sections were used per mouse. Sections were taken from the right and left medial corpus callosum.

$77.06 \pm 0.70\%$, $n=3$, $p=0.386$ when compared to the average across the sham cohort. Further, CCH mice demonstrated a significant decline in BCAS pericyte/microvessel coverage on day 3 compared to day 7 ($p=0.03$) and day 30 ($p=0.006$) CCH mice (Figure 6(d)).

PDGFRβ/ CD31 validation

PDGFRβ and CD13 co-stained on CD31 (vessels) DAPI positive nuclei in the corpus callosum on post-operative day 30 BCAS and sham specimens (Figures 4, 5, 6(a) and (b)).

There was no significant difference between pericyte coverage values of BCAS and sham animals on day 30 in the corpus callosum or the cortex when measured by either PDGFR β/CD31 ratio or CD13/CD31 ratio (Figure 5).

Discussion

The functional components of the brain vascular network (endothelium, pericytes, basement membrane) collectively regulate blood flow and transportation of nutrients to the astrocytes, microglia and neurons of the brain.[19] In the physiologic state these processes are controlled principally through vasoconstriction and dilatation.[13,20,21] Pericytes play a critical role in maintaining microvascular stability and luminal diameter, ultimately helping to ensure BBB integrity.[22–25] Mature pericytes are located in the perivascular space and embedded in the basement membrane with

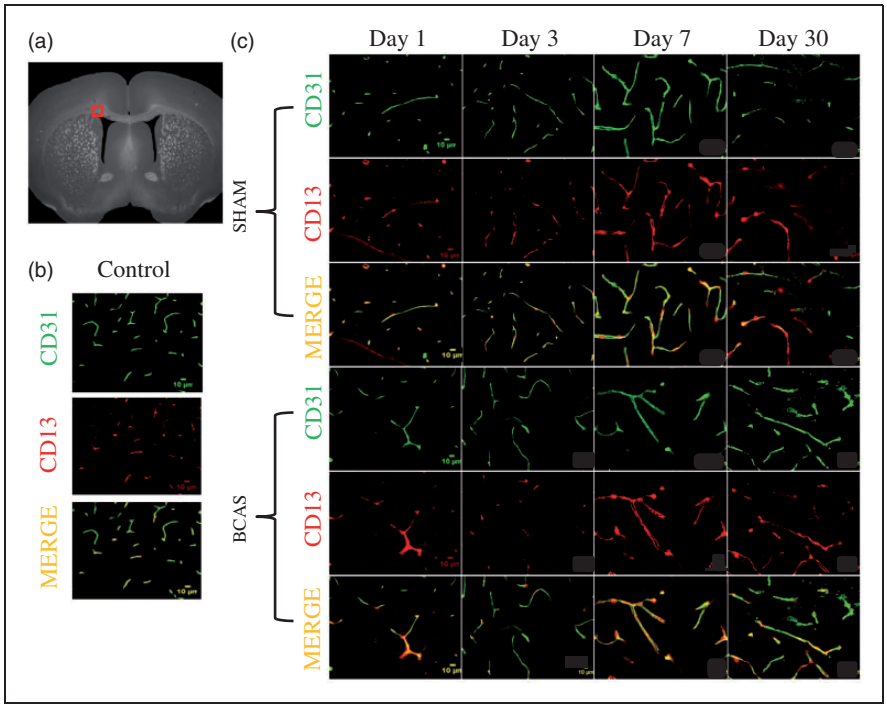

Figure 4. Pericyte response following BCAS. (a) Sections were obtained from the medial portion of the corpus callosum (b) Pericyte and vascular staining on control mice (no surgery). (c) Pericyte and vascular staining on sham and BCAS mice at days 1, 3, 7 and 30. Top: sham, bottom: BCAS. Green is CD 31, red is CD13 and yellow is merged. Scale bar: 10 μm.

endothelial cells and gap junctions.[11] Through a multitude of signaling pathways, pericytes have the capability to contract longitudinally and constrict or relax radially.[13] However, pericytes have not been shown to relax solely in response to increased blood flow and thus have been proposed to inhibit local reperfusion despite macro-resolution of an acute cerebrovascular insult.[13,26,27] Pericyte influence on vasoconstriction/dilation has also been estimated to contribute to 84% of a state-dependent change in CBF.[13] Collectively, it can be posited that pericytes are critically positioned to maintain a fine-tuned homeostasis in sensitive tissue.

In the setting of reduced CBF the neuronal stress response is rapid, leading to ATP release through damaged/compromised cell membranes and regulated pathways.[28,29] Pericytes exhibit a dynamic stress response to re-establish homeostasis of the NVU.[11] Prior reports suggest physiologic capillary pericyte coverage ratios ranging from 66% to 90% in the cortex.[30,31] However during pathological conditions such as AD, pericyte coverage has been shown to decrease, leading to BBB degradation and activation of complex molecular signaling pathways.[32] This study has attempted to extend this dysfunction to a CCH model. Under hypoxic conditions, pericytes detach from their perivascular locations allowing capillary permeability to molecules as large as 150 kDa (such as serum immunoglobulins), and toxic extravasation of plasma proteins.[14,22,23] Reductions in pericyte coverage in AD tissue correlate with extent of brain capillary leakage and BBB breakdown in both the cortex and hippocampus.[23,32] Pericyte contraction has been shown to play an essential role in obstructing capillary flow during cerebral ischemia.[13,27] Small vessel BBB dysfunction, and a resultant leakage of fluid and proteins, has been implicated in the pathogenesis of white matter lesions such as gliosis and demylination.[33,34]

Temporal CBF measurements have been previously studied in our BCAS model (0.18 mm microcoils) of CCH. CBF decreases by 33% within 2 h of the procedure and gradually recovers to near baseline by 30 days.[15] These results have been supported by Laser Speckle Flowmetry data.[35] Our study found significant BBB dysfunction in both the corpus callosum and cerebral cortex at day 3, with gradual recovery at day 7 and 30. Our data suggest that the most pronounced decreases in pericyte coverage and increases in BBB permeability evident on both Evans Blue extravasation studies and IgG staining (post-operative day 3) occur shortly after maximal CBF decreases (day 1). These changes occur in advance of white matter injury and cognitive dysfunction, which typically appear in this BCAS model on postoperative day 30, as demonstrated by our group and others.[15–18] Then, as the CBF measurements return towards normal, pericyte coverages and BBB permeability also normalize. This timeline

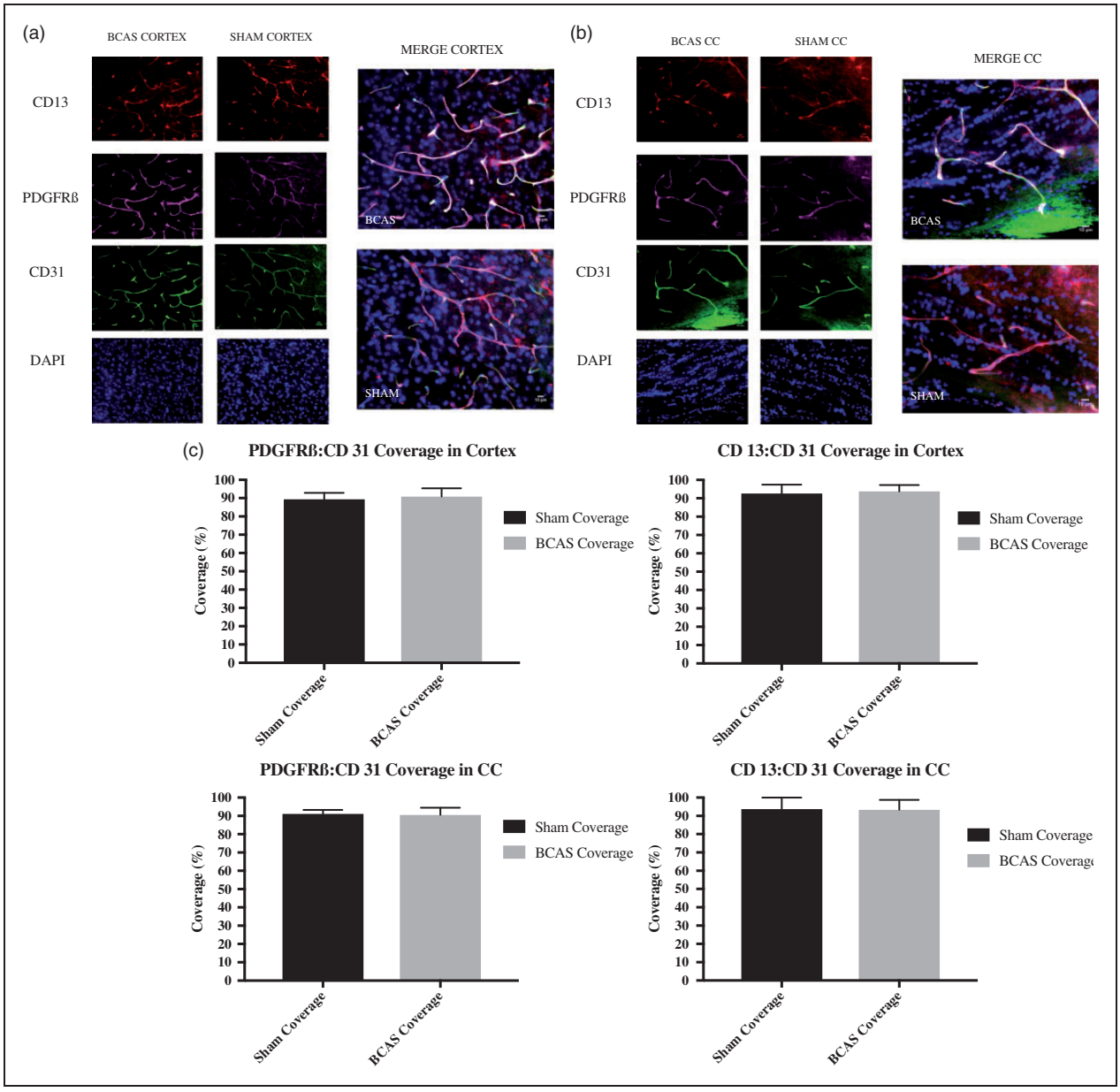

Figure 5. Pericyte response following BCAS in (a) cortex and (b) corpus callosum: co-localization of CD13 and PDGFRβ on day 30. Left: red is CD13, purple is PDGFRβ, green is CD31, and blue is DAPI. Right: co-localization of staining (white) on pericytes. Scale bar: 10 μm. Sections were obtained from the (a) frontal cortex and (b) medial portion of the corpus callosum. (c)Average ratio of PDGFRß:CD31 and CD13:CD31 coverage in the cortex and corpus callosum in BCAS and shams at day 30. Error bars represent standard error of the mean.

is logical, as CBF declines precede decreases in pericyte coverage and increases in BBB permeability, which in turn, precede histological white matter damage. The fact that temporary alterations in pericyte coverage and BBB permeability lead to subtle white matter ischemic changes and cognitive deficits is not surprising. Perhaps if the blood flow changes and BBB permeability increases were sustained at a more pronounced level, there would be more substantial white matter damage.

Extravasation of IgG has previously been demonstrated during neurological insults to the BBB.[36,37] The molecular weight of IgG (150 KD) is heavier than that of albumin-Evans blue complex (66 KD).[36] Although the BCAS cohort demonstrates visible IgG staining at day 3, our results suggest that IgG extravasation does not differ significantly between BCAS and shams across the time points.

This study sought to determine whether BBB components aside from pericytes, such as tight junction

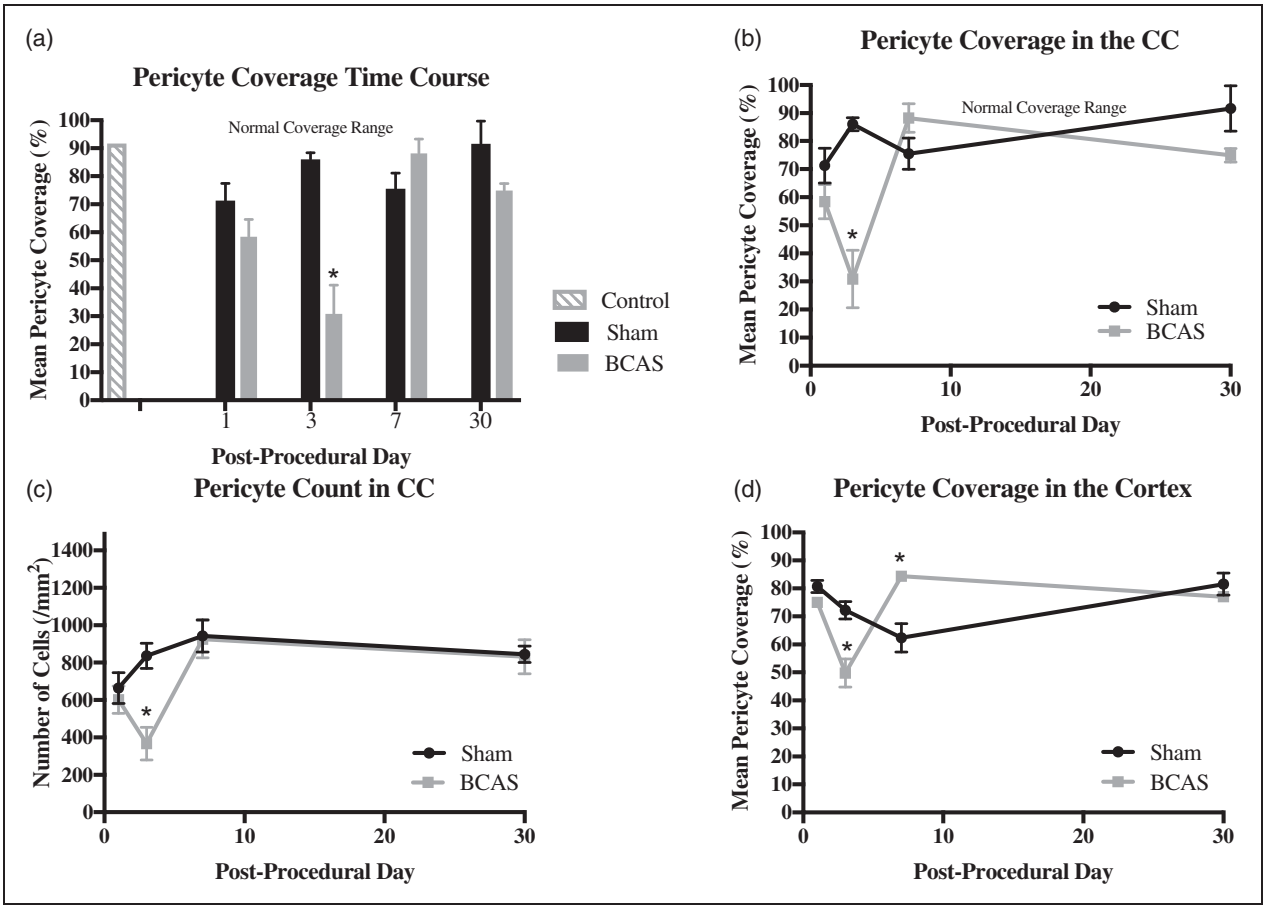

Figure 6. (a–c): Pericyte coverage and count in the corpus callosum. (a) Coverage bar graph. (b) Coverage time plot. (c) Count time plot. Values are depicted for BCAS and sham animals on days 1, 3, 7, 30. Two sections were used per mouse. Sections were taken from the right and left medial corpus callosum. (a–b) Controls ($n = 2$). BCAS pericyte coverage cohort (day 1, $n = 3$; day 3, $n = 3$; day 7, $n = 3$; day 30, $n = 3$). Sham pericyte coverage cohort (day 1, $n = 3$, day 3, $n = 4$; day 7, $n = 4$; day 30, $n = 4$). Day 3 BCAS values are significantly lower than values on day 7 and 30. Day 3 BCAS values are also significantly lower than mean values of the sham cohort at day 3. Shaded grey region depicts normal, physiologic cortical pericyte coverage values. * Signifies $p < 0.05$. Error bars represent standard error of the mean. (c) BCAS pericyte count cohort (day 1, $n = 3$; day 3, $n = 3$; day 7, $n = 3$; day 30, $n = 3$). Sham pericyte count cohort (day 1, $n = 3$; day 3, $n = 4$; day 7, $n = 4$; day 30, $n = 4$). Day 3 BCAS values are significantly lower than values on day 7 and 30. Day 3 BCAS values are also significantly lower than mean values of the sham cohort at day 3. (d) Pericyte coverage time plot in the cortex. Values are depicted for BCAS and sham animals on days 1, 3, 7 and 30. BCAS cohort (day 1, $n = 3$; day 3, $n = 3$; day 7, $n = 3$; day 30, $n = 3$). Sham cohort (day 1, $n = 3$; day 3, $n = 4$; day 7, $n = 4$; day 30, $n = 4$). Two sections were used per mouse. Sections were taken from the right and left cortex above the corpus callosum. Day 3 BCAS values are significantly lower than mean values of the sham cohort at day 3. Day 7 BCAS values are significantly increased compared to mean values of the sham cohort at day 7. *Signifies $p < 0.05$. Error bars represent standard error of the mean.

proteins, may contribute to the permeability changes evident in our CCH model. Occludin is an integral membrane protein located within the tight junction of endothelial cells, particularly within the BBB.[19] Previous studies show no changes in occludin levels after experimental CCH. Western blot analysis 24 and 48 h post-cerebral hypoperfusion demonstrates no change in ipsilateral and contralateral occludin expression.[38] Further, studies by Yang et al. reveal no changes in occludin percent coverages at days 1, 2 and 3 following cerebral hypoperfusion. Interestingly, relief of cerebral hypoperfusion results in occludin percent coverage declines, suggesting a protective effect under conditions of hypoperfusion.[39] Further, a rat BCAS model demonstrates increased Evans blue extravasation in the corpus callosum at post-operative day 3 and no changes in tight junction proteins occludin and claudin. This suggests that Evans blue escapes the blood vessel by a route exclusive of the tight junction complexes.[40] Consistent with these prior studies, our CCH mice (when compared to sham-operated animals) do not demonstrate any change in occludin coverage

in the corpus callosum at post-procedural days 1, 3, 7 and 30.

In this study, multiple antibodies were utilized to stain for pericytes. CD13 and PDGFRβ co-stained and confirmed the validity of each as a pericyte marker (Figure 5). Neither marker demonstrated decrease in pericyte coverage at day 30. Pericyte coverage values in our sham animals are consistent with normal physiologic measures reported in the literature.[30] Corpus callosum endothelial pericyte coverage is decreased significantly in the BCAS cohort on post-operative day 3. The decrease coincides temporally with BBB dysfunction and precedes the timeframe for pathological white matter injury.[15] There appears to be recovery (to a modest temporal peak) of pericyte coverage on day 7, concordant with the documented BBB restoration. Of note, there is also a reduction in cortical pericyte coverage and a corresponding increase in BBB permeability at these time points. The selective white matter damage characteristic of this BCAS model (lack of cortical damage despite BBB permeability) likely results from increased white matter vulnerability to ischemic injury rather than watershed distribution of the ischemia.[41–44] Further, variable time between Evans blue injection and culling can affect the results of evens blue extravasation. We limited this variability by completing euthanasia of the mice within 5 min after the 2-h Evans blue exposure.

Conclusion

Collectively, these findings indicate that CCH antagonizes NVU physiology and induces morphologic changes of angioarchitecture in the corpus callosum. The study demonstrates a substantial decrease in pericyte coverage following a relatively mild, sustained, ischemic insult. The pericyte response is temporally concordant with an increase in BBB permeability in the corpus callosum. Pericytes represent an important regulator of BBB integrity and a potential upstream target in efforts to ameliorate white matter injury in the setting of cerebral hypoperfusion.

Funding

The author(s) disclosed receipt of the following financial support for the research, authorship, and/or publication of this article: This research was supported by National Institute of Health grant ES024936 to WJM and Fondation Leducq Transatlantic Network of Excellence for the Study of Perivascular Spaces in Small Vessel Disease, ref no. 16 CVD 05.

Declaration of conflicting interests

The author(s) declared no potential conflicts of interest with respect to the research, authorship, and/or publication of this article.

Authors' contributions

QL performed the surgical experiments and tissue staining. RB performed tissue analysis and helped write the manuscript. RR performed tissue analysis and helped write the manuscript. AP performed tissue analysis and helped write the manuscript. DH performed tissue analysis and processing. PB performed tissue analysis and processing. ZZ designed the experiments and reviewed the manuscript. BZ designed and the experiments and reviewed the manuscript. WM designed the experiments and helped write the manuscript.

References

1. Durukan A and Tatlisumak T. Acute ischemic stroke: overview of major experimental rodent models, pathophysiology, and therapy of focal cerebral ischemia. *Pharmacol Biochem Behav* 2007; 87: 179–197.
2. Liu F and McCullough LD. Middle cerebral artery occlusion model in rodents: methods and potential pitfalls. *J Biomed Biotechnol* 2011; 2011: 464701.
3. Fine-Edelstein JS, Wolf PA, O'Leary DH, et al. Precursors of extracranial carotid atherosclerosis in the Framingham Study. *Neurology* 1994; 44: 1046–1050.
4. Heyer EJ, Sharma R, Rampersad A, et al. A controlled prospective study of neuropsychological dysfunction following carotid endarterectomy. Arch Neurol. 2002; 59: 217–222.
5. Ferri CP, Prince M, Brayne C, et al. Global prevalence of dementia: a Delphi consensus study. *Lancet* 2005; 366: 2112–2117.
6. Hebert LE, Weuve J, Scherr PA, et al. Alzheimer disease in the United States (2010-2050) estimated using the 2010 census. *Neurology* 2013; 80: 1778–1783.
7. Kalaria RN, Maestre GE, Arizaga R, et al. Alzheimer's disease and vascular dementia in developing countries: prevalence, management, and risk factors. *Lancet Neurol* 2008; 7: 812–826.
8. Rizzi L, Rosset I and Roriz-Cruz M. Global epidemiology of dementia: Alzheimer's and vascular types. *Biomed Res Int* 2014; 2014: 908915.
9. de la Torre JC. Is Alzheimer's disease a neurodegenerative or a vascular disorder? Data, dogma, and dialectics. *Lancet Neurol* 2004; 3: 184–190.
10. de la Torre JC. Alzheimer's disease is a vasocognopathy: a new term to describe its nature. *Neurol Res* 2004; 26: 517–524.
11. Muoio V, Persson PB and Sendeski MM. The neurovascular unit – concept review. *Acta Physiol* 2014; 210: 790–798.
12. Siegenthaler JA, Sohet F and Daneman R. 'Sealing off the CNS': cellular and molecular regulation of blood-brain barriergenesis. *Curr Opin Neurobiol* 2013; 23: 1057–1064.
13. Hall CN, Reynell C, Gesslein B, et al. Capillary pericytes regulate cerebral blood flow in health and disease. *Nature* 2014; 508: 55–60.
14. ElAli A, Theriault P and Rivest S. The role of pericytes in neurovascular unit remodeling in brain disorders. *Int J Mol Sci* 2014; 15: 6453–6474.

15. Shibata M, Ohtani R, Ihara M, et al. White matter lesions and glial activation in a novel mouse model of chronic cerebral hypoperfusion. *Stroke* 2004; 35: 2598–2603.
16. Liu Q, He S, Groysman L, et al. White matter injury due to experimental chronic cerebral hypoperfusion is associated with C5 deposition. *PLoS One* 2013; 8: e84802.
17. Shibata M, Yamasaki N, Miyakawa T, et al. Selective impairment of working memory in a mouse model of chronic cerebral hypoperfusion. *Stroke* 2007; 38: 2826–2832.
18. Ihara M and Tomimoto H. Lessons from a mouse model characterizing features of vascular cognitive impairment with white matter changes. *J Aging Res*. 2011; 2011: 978761.
19. Zlokovic BV. The blood-brain barrier in health and chronic neurodegenerative disorders. *Neuron* 2008; 57: 178–201.
20. Fernandez-Klett F, Offenhauser N, Dirnagl U, et al. Pericytes in capillaries are contractile in vivo, but arterioles mediate functional hyperemia in the mouse brain. *Proc Natl Acad Sci U S A* 2010; 107: 22290–22295.
21. Peppiatt CM, Howarth C, Mobbs P, et al. Bidirectional control of CNS capillary diameter by pericytes. *Nature* 2006; 443: 700–704.
22. Armulik A, Genove G, Mae M, et al. Pericytes regulate the blood-brain barrier. *Nature* 2010; 468: 557–561.
23. Bell RD, Winkler EA, Sagare AP, et al. Pericytes control key neurovascular functions and neuronal phenotype in the adult brain and during brain aging. *Neuron* 2010; 68: 409–427.
24. Chan-Ling T, Page MP, Gardiner T, et al. Desmin ensheathment ratio as an indicator of vessel stability: evidence in normal development and in retinopathy of prematurity. *Am J Pathol* 2004; 165: 1301–1313.
25. Daneman R, Zhou L, Kebede AA, et al. Pericytes are required for blood-brain barrier integrity during embryogenesis. *Nature* 2010; 468: 562–566.
26. Attwell D, Buchan AM, Charpak S, et al. Glial and neuronal control of brain blood flow. *Nature* 2010; 468: 232–243.
27. Yemisci M, Gursoy-Ozdemir Y, Vural A, et al. Pericyte contraction induced by oxidative-nitrative stress impairs capillary reflow despite successful opening of an occluded cerebral artery. *Nat Med* 2009; 15: 1031–1037.
28. Juranyi Z, Sperlagh B and Vizi ES. Involvement of P2 purinoceptors and the nitric oxide pathway in [3H]purine outflow evoked by short-term hypoxia and hypoglycemia in rat hippocampal slices. *Brain Res* 1999; 823: 183–190.
29. Melani A, Turchi D, Vannucchi MG, et al. ATP extracellular concentrations are increased in the rat striatum during in vivo ischemia. *Neurochem Int* 2005; 47: 442–448.
30. Winkler EA, Bell RD and Zlokovic BV. Pericyte-specific expression of PDGF beta receptor in mouse models with normal and deficient PDGF beta receptor signaling. *Mol Neurodegener* 2010; 5: 32.
31. Ben-Zvi A, Lacoste B, Kur E, et al. MSFD2A is critical for the formation and function of the blood brain barrier. *Nature* 2014; 509: 507–511.
32. Sengillo JD, Winkler EA, Walker CT, et al. Deficiency in mural vascular cells coincides with blood-brain barrier disruption in Alzheimer's disease. *Brain Pathol* 2013; 23: 303–310.
33. Caplan LR. Dilatative arteriopathy (dolichoectasia): what is known and not known. *Ann Neurol* 2005; 57: 469–471.
34. Pico F, Labreuche J, Touboul PJ, et al. Intracranial arterial dolichoectasia and small-vessel disease in stroke patients. *Ann Neurol* 2005; 57: 472–479.
35. Maki T, Ihara M, Fujita Y, et al. Angiogenic and vasoprotective effects of adrenomedullin on prevention of cognitive decline after chronic cerebral hypoperfusion in mice. *Stroke* 2011; 42: 1122–1128.
36. Kuang F, Wang B-R, Zhang P, et al. Extravasation of blood-borne immunoglobulin G through blood-brain barrier during adrenaline-induced transient hypertension in the rat. *Int J Neurosci* 2004; 114: 575–591.
37. Armulik A, Genové G, Mäe M, et al. Pericytes regulate the blood-brain barrier. *Nature* 2010; 468: 557–561.
38. ElAli A, Thériault P, Préfontaine P, et al. Mild chronic cerebral hypoperfusion induces neurovascular dysfunction, triggering peripheral beta-amyloid brain entry and aggregation. *Acta Neuropathol Commun* 2013; 1: 75.
39. Yang F, Zhang X, Sun Y, et al. Ischemic postconditioning decreases cerebral edema and brain blood barrier disruption caused by relief of carotid stenosis in a rat model of cerebral hypoperfusion. *PloS One* 2013; 8: e57869.
40. Sood R, Yang Y, Taheri S, et al. Increased apparent diffusion coefficients on MRI linked with matrix metalloproteinases and edema in white matter after bilateral carotid artery occlusion in rats. *J Cereb Blood Flow Metab* 2009; 29: 308–316.
41. Pantoni L, Garcia JH and Gutierrez JA. Cerebral white matter is highly vulnerable to ischemia. *Stroke* 1996; 27: 1641–1647.
42. Chalela JA, Wolf RL, Maldjian JA, et al. MRI identification of early white matter injury in anoxic–ischemic encephalopathy. *Neurology* 2001; 56: 481–485.
43. Wakita H, Tomimoto H, Akiguchi I, et al. Axonal damage and demyelination in the white matter after chronic cerebral hypoperfusion in the rat. *Brain Res* 2002; 924: 63–70.
44. Stys PK. Anoxic and ischemic injury of myelinated axons in CNS white matter: from mechanistic concepts to therapeutics. *J Cereb Blood Flow Metab* 1998; 18: 2–25.